Performance of a 12-Kilometer Photonic Link for X-Band Antenna Remoting in NASA's Deep Space Network

W. Shieh,[1] G. Lutes,[1] S. Yao,[1] L. Maleki,[1] and J. Garnica[2]

This article reports on a field demonstration of fiber-optic downlink antenna remoting at 8.4 GHz (X-band) over 12 km in NASA's Deep Space Network (DSN). In this demonstration, we compare the noise temperature and linearity of a present-day receiver configuration with that of a receiver in a which a 12-km advanced analog microwave fiber-optic link is inserted between the low-noise amplifier (LNA) and the downconverter. The test results showed no significant difference in noise temperature and linearity between the two systems. This capability can make the received radio frequency signals available to any location in a complex and enables remoting the entire receiver and its associated equipment, with the exception of the LNA.

I. Introduction and Background

Prior to 1990, 7/8-inch-diameter air dielectric coaxial cables carried intermediate frequency (IF) signals over the 100 m from the antenna to the control room at Deep Space Station 13 (DSS 13) in the NASA Deep Space Communications Complex (DSCC) at Goldstone in California's Mohave Desert. Because of the high loss and delay instability of these coaxial cables, they were replaced in 1990 with the highest performance analog fiber-optic links available at the time. However, the bandwidth on these links was limited to about 1 GHz, which precluded their use at the radio frequencies. As a result of this bandwidth limitation, it was necessary to have the downconverters and associated equipment, such as the local oscillators, in the antenna area near the low-noise amplifier (LNA).

We performed a study in early 1990 and found that microwave fiber-optic technology had advanced to a level that would enable high-fidelity, high-dynamic-range analog fiber-optic links to operate at microwave frequencies. This led to a proposal to demonstrate such a link [1] for possible use in remoting the downlink of a Deep Space Network (DSN) receiver. The proposal was funded, and the first successful demonstration of 8.4-GHz (X-band) receiver downlink remoting in the DSN was performed in 1994 [2]. This was a 1-day feasibility test that, with the exception of dynamic range, met all of the requirements of the receiver system.

This demonstration left a number of engineering problems and questions to be resolved. First, the link employed a Nd: YAG laser, which had a typical low-frequency relative-intensity-noise (RIN) peak

[1] Tracking Systems and Applications Section.

[2] TMOD Engineering Program Office.

that was modulated into the radio frequency (RF) signal passband. This resulted in degradation of the dynamic range of the receiver system when used in conjunction with a less than ideal optical modulator. The laser also proved to be unreliable because of poor fabrication techniques used by the manufacturer. Second, the external optical modulator had a high half-wave voltage (V_π) and high optical loss. This contributed to insufficient dynamic range.

Recent improvements in lasers and optical modulators led us to this demonstration of full-performance downlink antenna remoting over a 12-km distance at the received 8.4-GHz (X-band) frequency. This system meets all of the noise-temperature and dynamic-range requirements of the DSN receiver system.

A block diagram of this demonstration is provided in Fig. 1. A received 8.4-GHz RF signal from the antenna is applied to the LNA, where it is amplified and then split with an RF power splitter into two RF signals. One signal follows the normal path for a DSN receiver (IF remoting link). A downconverter converts this signal to a relatively low intermediate frequency (<500 MHz), which then is transmitted to the control room over a 100-m-long analog fiber-optic link having a frequency response of 1 GHz. Here it is connected to one port of a switch. The other signal from the RF power splitter is transmitted with a high-performance analog microwave fiber-optic link directly from the LNA to the control room over 12 km of optical fiber (RF remoting link). In the control room, a second downconverter converts this signal to IF. This signal then is connected to the other port of the switch. The output of the switch is connected to the instrumentation used to measure the system noise temperature and linearity. By switching between the two signals, station personnel can compare them.

II. Advantages of Remoting

The advantage this capability offers is that the received RF signals from any antenna can be made available at any location within a DSCC. This capability has the potential to greatly enhance the performance, flexibility, and reliability of a DSCC and, at the same time, lower operating and hardware costs.

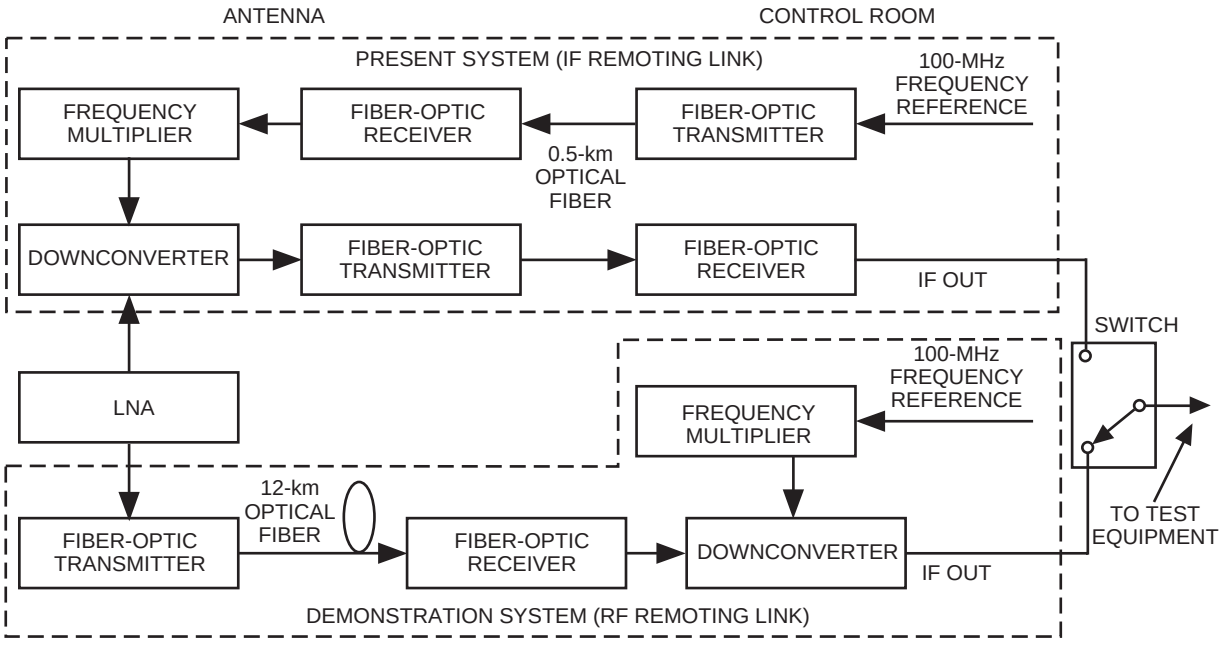

Fig. 1. Block diagram of the demonstration configuration.

This capability permits the downconverters and related equipment to be moved out of the antenna area to a remote command and signal processing center (SPC). This is a lot of equipment when you consider that a DSS can have as many as seven downconverters. If this equipment from all of the antennas in a complex were co-located at the SPC, it would facilitate the servicing of it by reducing the need to travel between DSSs. It would enable a single set of hot spares to back up all of the downconverters and associated equipment in a complex. As a result, this could greatly reduce down time for this equipment. Some functions, like the multiplier in the local oscillator (LO) chain, could be shred by all of the receivers in the complex, thus reducing the amount of hardware.

Radio astronomers would be able to make radiometer measurements on the received microwave signals from the SPC without the need for a downconverter.

If antenna remoting were to be combined with an optical matrix switch, an entire DSCC could operate as a single system with the capability to be reconfigured quickly in a myriad of ways. For instance, antennas could be RF arrayed to increase the aperture for higher resolution or to increase the collection area for higher sensitivity. In the case of antenna failures, the antennas could be spared on a priority basis.

III. Fiber-Optic Link Design

We designed the microwave fiber-optic link used in this demonstration to be placed between the LNA and the downconverter and to meet the noise and dynamic-range requirements of a DSN receiver. The goal was to extend the length of the microwave signal path to 12 km without measurably degrading the noise and dynamic range of the receiving system in which the photonic link is embedded.

To prove that the goals were met, we installed a capability to switch between the output of the present receiver and the output of the receiver with the extended signal path. Engineers at the station were challenged to tell which configuration the system was in by observing and measuring the received signals.

The noise power at the input to the receiver is

$$P_{\text{in}} = (k \times T \times B) \tag{1}$$

where k, T, and B are Boltzmann's constant, the noise temperature of the LNA, and the noise bandwidth of the system, respectively.

The equivalent noise power at the output of a linear system is

$$P = G_A \times P_{\text{in}} \tag{2}$$

where G_A is the system gain.

The nonlinear gain of an electronic system can be expressed as

$$G = \frac{G_A}{1 + a\left(\dfrac{P}{P_{1\text{dB}}}\right)} \tag{3}$$

where

$G_A =$ the linear gain

$G_c = 0.8G_A =$ the nonlinear gain at the 1-dB compression point

$a = \dfrac{G_A}{G_c} - 1 = 0.25$, a constant based on 1-dB compression

$P_{1\text{dB}} =$ the output 1-dB saturation power of the fiber-optic link

From Eqs. (2) and (3), the power output, P_o, of a nonlinear system is

$$P_o = \frac{G_A \times P_{\text{in}}}{1 + 0.25\dfrac{P}{P_{1\text{dB}}}} \tag{4}$$

For small nonlinearities,

$$P_o \approx G_A P_{\text{in}} \left(1 - 0.25\frac{P}{P_{1\text{dB}}}\right) \approx G_A P_{\text{in}} - 0.25\frac{(G_A P_{\text{in}})^2}{P_{1\text{dB}}} \tag{5}$$

Taking the derivative of Eq. (5),

$$\frac{dP_o}{dP_{\text{in}}} \approx G_A - 0.5\frac{P}{P_{1\text{dB}}} \tag{6}$$

Given the maximum allowable nonlinearity and using the nonlinear term from Eq. (6), the minimum 1-dB saturation level is

$$P_{1\text{dB}} \approx 0.5 \times \frac{P}{NL} \tag{7}$$

where NL is the nonlinearity of the system, defined as $G_A - (dP_o/dP_{\text{in}})$. It was suggested by C. T. Stelzried that the nonlinearity of the photonic link should be limited to $NL = 0.2$ percent. From Eqs. (2) and (7) for $G_A = 1000, B = 1.5 \times 10^8$ Hz, and $T = 300$ K, the maximum output signal level, in dB, without exceeding 0.2 percent nonlinearity on the photonic link, is

$$P_{1\text{dB}} \approx 10 \times \log\left(0.5 \times \frac{G_A \times K \times T \times B}{0.002}\right) = -38 \text{ dBm} \tag{8}$$

As shown in Fig. 2(a), the demonstration microwave fiber-optic link contains a preamplifier with a noise temperature, T_{pre}, and a gain, G_{pre}. The preamplifier drives an external optical modulator that modulates the optical carrier generated by a semiconductor laser diode. The noise temperature at the modulator input is T_p, and the gain from the input of the modulator to the output of the photodiode is G_{op}. There is a 12-km-long optical fiber between the modulator and the photodetector. The noise temperature of the fiber-optic link is

$$T_{fo} = T_{pre} + \frac{T_p}{G_{pre}} \tag{9}$$

The 12-km microwave fiber-optic link is inserted between the LNA and the downconverter, as shown in Fig. 2(b).

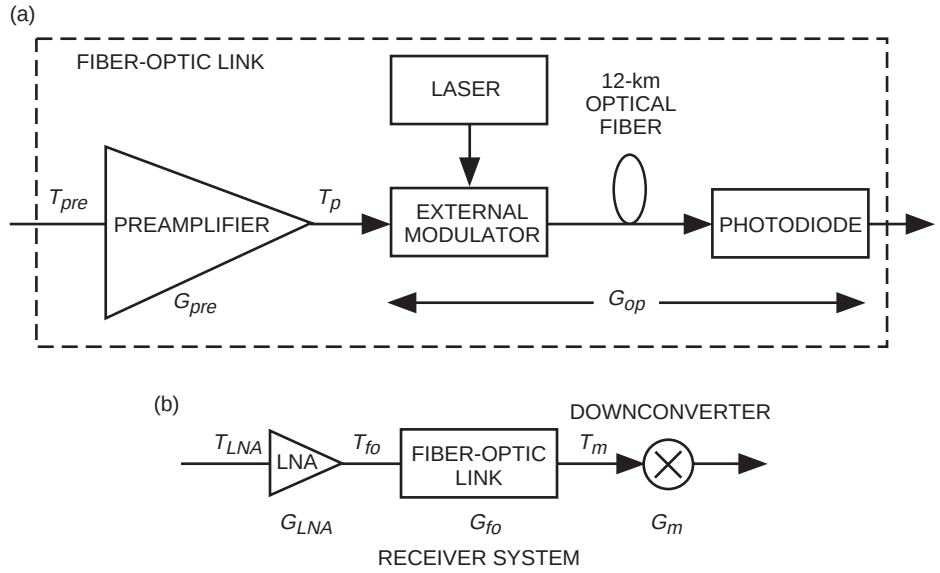

Fig. 2. Block diagrams of (a) the high-performance microwave fiber-optic link and (b) the overall remote receiver downlink system, showing the placement of the fiber-optic link. The noise temperature and gain designations used in the analysis are shown in both figures for clarity.

The noise temperature of the remoted receiver system is

$$T_T = T_{LNA} + \frac{T_{fo}}{G_{LNA}} + \frac{T_m}{G_{LNA} \times G_{fo}} \tag{10}$$

where T_{LNA}, T_{fo}, and T_m are the noise temperatures of the LNA, the fiber-optic link, and the downconverter, respectively, and G_{LNA} and G_{fo} are the gains of the LNA and the fiber-optic link, respectively. It can be seen from Eqs. (4) and (5) that the fiber-optic link noise contribution is small if the gains of the LNA and preamplifier are large.

In our system, the preamplifier has enough gain, ≈60 dB, to give a fiber-optic link gain of 15 dB. Because of the extra 15 dB of gain between the LNA and the downconverter, the system noise temperature is slightly lower for the demonstration system.

IV. Components and Characteristics

Because at the time there were no available commercial high-performance X-band analog fiber-optic links that would meet our requirements, we purchased the component parts from different sources and assembled the photonic link in our laboratory. The transmitter consists of a 1.5-μm-wavelength semiconductor laser followed by a high-performance Mach–Zehnder optical modulator. A proprietary modulator bias circuit was designed and fabricated. It was used to eliminate the modulator bias drift problem associated with the proton-exchange technology used to fabricate the modulator. The RF port of the modulator is driven by a three-stage preamplifier having a 60-dB gain. This results in a fiber-optic link gain of 15 dB and reduces noise generated in the optical path.

The laser was biased at 250 mA and emitted about 25 mW of optical power. The modulator has a V_π of about 25 V at 8.4 GHz and an insertion loss of about 3 dB. An additional 60-dB optical isolator was placed after the modulator to avoid any ill effects due to reflections in the system. The optical power at the output of the optical transmitter was 6.11 mW.

We used 12 km of bare Corning SMF-28 optical fiber between the fiber-optic transmitter and receiver to simulate the cable between two stations located 12 km apart. The receiver is a 15-GHz PIN photodiode detector with a responsivity of about 0.8 mA/mW. The detected photocurrent at the output of the receiver was 2.2 mA.

The measured $P_{1\mathrm{dB}}$ of the photonic link is about −37 dBm, which meets the linearity requirement. Because the fiber-optic link provides an additional gain of 15 dB before the downconverter, the system noise temperature in the demonstration receiver is slightly lower than that of the present receiver.

Figure 3 shows the phase noise of the demonstration fiber-optic link normalized to the 1-Hz bandwidth as a function of offset frequency from the 8.4-GHz carrier. The measurement system phase noise also is shown.

Figure 4 shows the relative-intensity-noise (RIN) spectrum of the laser. It can be seen that the RIN is larger when measured at the end of the 12-km fiber-optic cable. This is due to phase modulation (PM)-to-amplitude modulation (AM) conversion resulting from the dispersion in the optical fiber. It also can be shown that the RIN has a relaxation resonance peak around 10 GHz, which is near the operating frequency. In spite of this, the microwave fiber-optic link still meets the dynamic range requirement. The dynamic range of the link could be improved somewhat at X-band by using a laser with the relaxation resonance peak in a different frequency range.

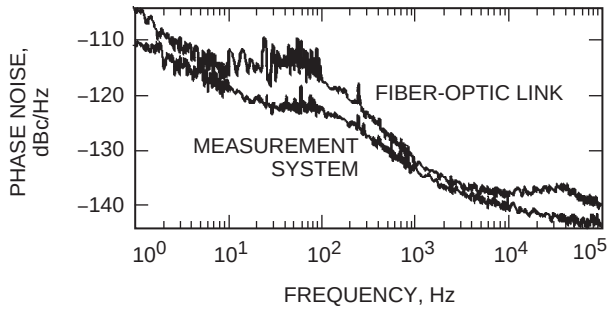

Fig. 3. The carrier phase noise of the fiber-optic link used in the demonstration and the measurement system noise floor.

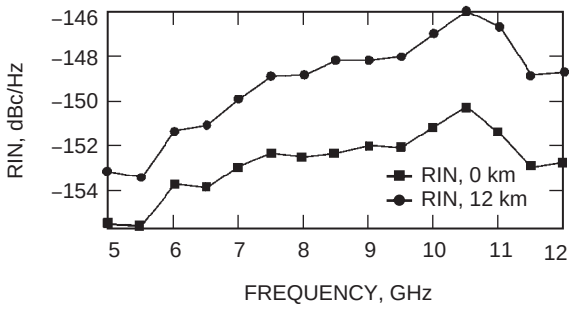

Fig. 4. The measured RIN of the laser for a short link and a 12-km link. The RIN is increased in the 12-km link by the PM-to-AM conversion resulting from dispersion in the optical fiber.

The RIN of the laser is impressed on an RF signal that is transmitted in the fiber-optic link. Figure 5 shows a plot of this noise on an 8.4-GHz signal for a short link and for the 12-km link. The plots show that the upconverted RIN also is larger after the signal passes through the 12-km optical fiber. This effect can be reduced by operating near the 1.3-μm zero-dispersion wavelength of normal fiber by using either dispersion-shifted fiber or dispersion compensation. However, fiber loss is higher at 1.3 μm, so use of this wavelength will reduce the usable transmission distance.

Station personnel sporadically perform system operating noise temperature, T_{op}, and linearity tests on the two receiver systems using the radiometer calibration method developed by C. T. Stelzried and M. J. Klein [3,4].

The optical power and link gain of the demonstration system have remained stable, as they have in the present signal path. The demonstration system consistently exhibited slightly better system operating noise temperature and nonlinearity of 0.2 to 0.5 percent, which agrees with the system design. The following table shows an example of the "precal" measurements taken on June 12, 1998. A precal measurement is one of several radiometer measurements that are made in a series and averaged to obtain

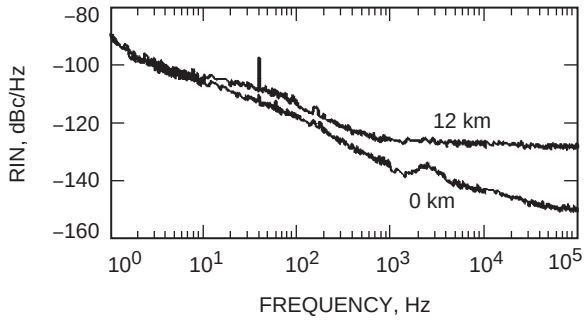

Fig. 5. The carrier RIN noise at 8.4 GHz, again showing the increased noise resulting from dispersion in the optical fiber.

a statistically significant result. In the example, there are three pairs of precals, and the results are presented side by side for comparison purposes. The measurements for the demonstration system and the present system were taken 5 minutes apart.

Parameter	Sample		
	Precals I (demonstration/present)	Precals II (demonstration/present)	Precals III (demonstration/present)
T_{op}, K	41.8/42.0	41.5/42.0	41.5/41.8
Nonlinearity, percent	0.07/0.03	0.28/0.32	0.23/0.34

We also tracked a Mars Global Surveyor (MGS) signal using both systems and compared the results. There were no observable differences between the IF spectra of the two systems.

V. Conclusion

In summary, we have demonstrated downlink X-band antenna remoting at DSS 13 over a distance of 12 km. We compared the demonstration system with the present system and observed no significant difference in noise temperature and linearity.

This demonstration is important because it proves that the RF signals from the antennas in a DSCC can be made available anyplace within a complex. This ability can result in significant improvements in flexibility and reliability of a DSCC.

There is no reason this capability cannot be extended to 20 to 40 GHz (Ka-band) in the future. It is within the capability of modern state-of-the-art photonic devices that are being demonstrated in laboratories around the world.

We could improve the dynamic range of the remoted receiver beyond that of the present receiver by the use of higher-power lasers, control of the frequency of the relaxation resonance peak, and use of dispersion compensation.

Acknowledgments

The authors would like to thank C. Stelzried for his help in understanding the characterization of the operating noise temperature and linearity of the receiver systems in the DSN; L. Rauch for his suggestion and support for having a demonstration of a remote receiver downlink; J. Dick for enlightening discussions; and G. Bury, J. Crook, G. Farner, and other DSS-13 station personnel, who assisted in the demonstration.

References

[1] R. T. Logan, Jr., G. F. Lutes, and L. Maleki, "Microwave Analog Fiber-Optic Link for Use in the Deep Space Network," *The Telecommunications and Data Acquisition Progress Report 42-100, October–December 1989*, Jet Propulsion Laboratory, Pasadena, California, pp. 21–33, February 15, 1990.
http://tmo.jpl.nasa.gov/tmo/progress_report/42-100/100C.pdf

[2] X. S. Yao, G. Lutes, R. T. Logan, and L. Maleki, "Field Demonstration of X-Band Photonic Antenna Remoting in the Deep Space Network," *The Telecommunications and Data Acquisition Progress Report 42-117, January–March 1994*, Jet Propulsion Laboratory, Pasadena, California, pp. 29–34, May 15, 1994.
http://tmo.jpl.nasa.gov/tmo/progress_report/42-117/117c.pdf

[3] C. T. Stelzried and M. J. Klein, "Precision DSN Radiometer Systems: Impact on Microwave Calibrations," *Proceedings of the IEEE*, vol. 82, no. 5, pp. 776–787, May 1994.

[4] C. T. Stelzried and M. J. Klein, "Corrections to 'Precision DSN Radiometer Systems: Impact on Microwave Calibration,'" *Proceedings of the IEEE*, p. 1187, August 1996.